Cardiovascular Engineering and Technology, Vol. 10, No. 2, June 2019 *(© 2019)* pp. 344–353
https://doi.org/10.1007/s13239-019-00413-6

Mechanics of Atherosclerotic Plaques: Effect of Heart Rate

Mehrdad Zareh, Ramsey Katul, and Hadi Mohammadi

The Heart Valve Performance Laboratory, School of Engineering, Faculty of Applied Science, University of British Columbia, Kelowna, BC V1V 1V7, Canada

(Received 5 January 2019; accepted 28 March 2019; published online 4 April 2019)

Associate Editor Ajit P. Yoganathan oversaw the review of this article.

Abstract

Purpose—Atherosclerotic plaques are highly heterogeneous, nonlinear materials with uncharacteristic structural behaviors. It is well known that mechanics of atherosclerotic plaques significantly depend on plaque geometry, location, composition, and loading conditions. There is no question that atherosclerotic plaques are viscoelastic. Plaques are characterized as the buildup of low-density lipoprotein cholesterol, macrophages, monocytes, and foam cells at a place of inflammation inside arterial walls. Lipid core and fibrous cap are the two major ingredients that are frequently used for the identification of main constituting quantities of atherosclerotic plaques. The lipid core contains of debris from dead cells, esterified cholesterol and cholesterol crystals. The fibrous cap contains smooth muscle cells and collagen fibers. All these materials contribute to the viscoelastic properties of atherosclerotic plaques. Computational studies have shown great potential to characterize this mechanical behavior. Different types of plaque morphologies and mechanical properties have been used in a computational platform to estimate the stability of rupture-prone plaques and detect their locations. In this study for the first time to the best of authors' knowledge, we hypothesize that heart rate is also one of the major factors that should be taken into account while mechanics of plaques is studied.

Method—We propose a tunable viscoelastic constitutive material model for the fibrous cap tissue in order to calculate the peak cap stress in normal physiological (dynamic) conditions while heart rate changes from 60 bpm to 150 bpm in 2D plane stress models. A critical discussion on stress distribution in the fibrous cap area is made with respect to heart rate for the first time.

Results—Results strongly suggest the viscoelastic properties of the fibrous cap tissue and heart rate together play a major role in the estimation of the pick cap stress values.

Conclusions—The results of current study may provide a better understanding on the mechanics of vulnerable atherosclerotic plaques and that any experimental methods assessing the viscoelasticity of plaque composition during progression are highly desirable.

Keywords—Atherosclerotic plaque, Plaque vulnerability, Plaque instability, Pulsatile flow, Finite element method, Viscoelasticity, Heart rate.

INTRODUCTION

Acute myocardial infarction (AMI) is caused by coronary thrombosis, which is mainly due to the rupture of vulnerable plaques. Plaques with vulnerable morphology are located at multiple sites on the coronary tree. Thus, accurately identifying plaques with the highest risk of rupture is of crucial importance. The detection of vulnerable plaques prior to rupture would considerably reduce the occurrences of AMI. Despite substantial efforts towards the early detection and therapy of unstable coronary plaques, AMI still remains the leading cause of death worldwide.[5,9,11] Computational approaches have been extensively applied on two-dimensional (2D) or three-dimensional (3D) imaging modalities in order to estimate the peak cap stress (PCS) in the fibrous cap area using mostly the finite element method (FEM).[2,4,6,13,16] This evaluated PCS is then compared to the "gold standard" of 300 kPa in order to determine the stability of rupture-prone plaques.[16] Plaque morphology, i.e., necrotic core size, fibrous cap thickness and so on, loading and boundary conditions, and plaque composition are known to be significantly influential in PCS.[4,6,13,15,16] Constitutive material models applied in mechanical models of plaques have a wide range from simplistic, 2D linear and isotropic material models[18] to more sophisticated, 3D hyperelastic and anisotropic material models.[4,8,13,15] The problem with all of these material models is that none of them account for the viscous properties of the fibrous cap tissue, with the exception

Address correspondence to Hadi Mohammadi, The Heart Valve Performance Laboratory, School of Engineering, Faculty of Applied Science, University of British Columbia, Kelowna, BC V1V 1V7, Canada. Electronic mail: hadi.mohammadi@ubc.ca

of a couple of fairly recent studies.[10,19] It is well known that thin fibrous caps are severely inflamed and the percentage of macrophage density is as high as ~ 14%,[9] which is even higher (> 26%) for ruptured plaques. Since the fibrous cap tissue is thin, their ability to accommodate macrophages is very low. Also, apoptosis in the fibrous cap tissue is limited to macrophages alone. This is due to the amount of vascular smooth muscle cells (SMCs) decreasing to nothing throughout plaque progression until rupture occurs.[12] In other words, change in macrophages and SMCs density leads to change in viscous properties of the fibrous cap tissue. Given the viscous nature of the thin fibrous cap area, heart rate (HR) is hypothesized to play a major role in assessing PCS. In fact, to date, to the best of the authors' knowledge, in almost all of the studies performed around the hemodynamics, a heart rate (HR) of 70–72 beats per minute (bpm) has been considered. In fact, the HR of ~ 72 bpm does not represent the entire normal physiological conditions under which the cardiovascular system functions. In some cases, such as resting, sleeping, *etc.*, HR could be as low as 60 bpm. In contrast, HR can increase to even 150 bpm while jogging, running, etc. Also, daily emotional conditions such as anxiety and stress may affect our HR. Therefore, a HR range of 60–150 bpm seems to be justifiable as normal HR conditions under which our cardiovascular system performs. In this study, a tunable viscoelastic constitutive material model is proposed to computationally assess PCS in the fibrous cap tissue with respect to HR in a 2D computational platform. We developed a finite element platform which is solved by Mechanical APDL 2015 running on an Intel® Core™ 2 Duo T6670 @ 2.2 GHz and 2.00 GB of RAM.

METHODS

Geometrical Models

Two groups of geometrical models are considered in this study: (1) idealistic models as presented in Fig. 1,[15,19] and (2) realistic models obtained from varying imaging modalities, such as optical coherence tomography (OCT), intravascular ultrasound, (IVUS) and histology,[8] as shown in Fig. 2. Two critical cap thicknesses are considered for idealistic models: 70 and 100 μm. The outer diameter of the coronary artery in all models is set to 3.3 mm.[15,19]

Idealistic Models

Four representative IVUS images are carefully selected to represent the geometry of the thin fibrous cap tissue. This geometry is then categorized into three types: nodal (Fig. 1a), linear (Fig. 3c), and curve-linear (Fig. 1d). In all of these models, cap thickness is set to 70 and 100 μm and the diameter of plaque is set to 3.3 mm (Fig. 1). Using these IVUS images, three idealistic 2D models are generated corresponding to each category: nodal (Fig. 1e), linear (Fig. 1f) and curve-linear (Fig. 1g). A random geometry of a 2D realistic

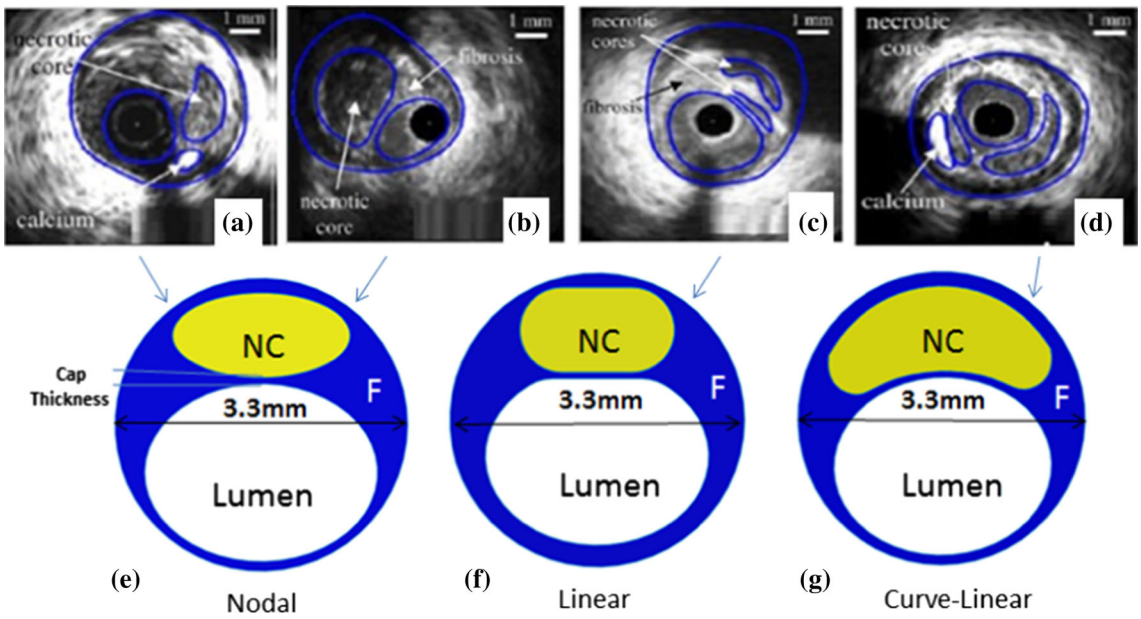

FIGURE 1. (a–d) Selected IVUS images which are the representative of all types of plaque morphologies[14] (@ 2014 World Scientific Publishing Co., Inc. adapted with permission). This classification is based on the geometry of the fibrous cap which is considered to be: nodal (a), linear (b, c), and curve-linear (d), and the corresponding idealistic models are defined as: e (nodal), f (linear) and g (curve linear). Cap thickness = 70 and/or 100 μm); F, fibrous cap; NC, necrotic core.

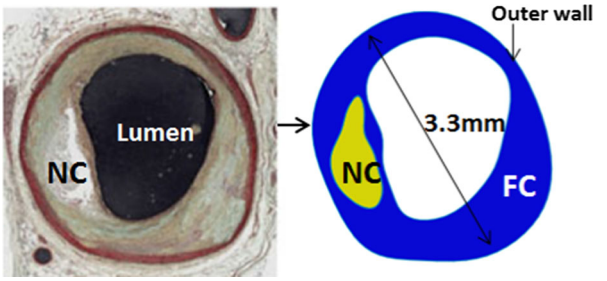

FIGURE 2. This figure shows a typical geometrical model (right) developed on a histology image of an atherosclerotic plaque,[1] *NC* necrotic core, *FC* fibrous cap.

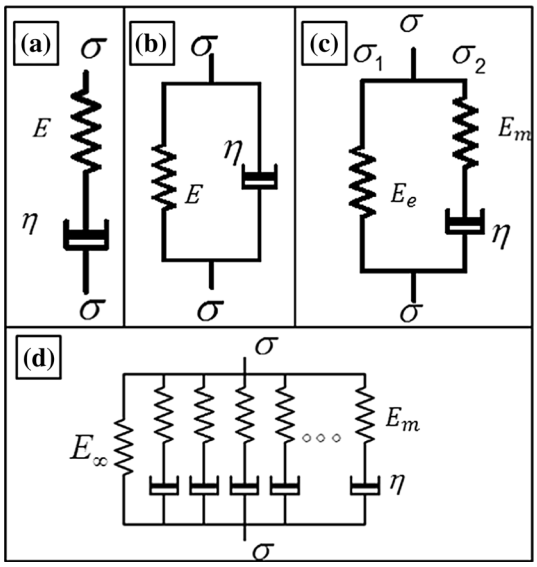

FIGURE 3. Illustration of the linear physical models used to describing behaviour of viscoelastic materials. (a) Maxwell Model; (b) Kelvin-Voight Model; (c) Standard Linear Solid; (d) Wiechert Model. *E* and *η* refers to elastic and viscous part of the model, respectively. E_∞ and E_m refers to the elasticity at infinite time and elasticity of Maxwell arm, respectively. *σ* represents the stress (load) imposed on the system.

plaque can be created by one or a combination of two or three of these idealistic models.

Idealistic Models

These models are produced using imaging techniques such as IVUS and OCT and histology images and then are digitized using AutoDesk (2017i) CAD software. A typical geometrical model for plaque is illustrated in Fig. 2.

Numerical Procedure

The stress tensor of linear viscoelasticity is stated with respect to the strain history as such:

$$\sigma^*(t) = \int_{-\infty}^{t} \tau(t-s)\varepsilon(\dot{s})\mathrm{ds} \tag{1}$$

$$\varepsilon = \nabla u + \nabla u^T \tag{2}$$

$$\dot{\varepsilon} = \nabla v + \nabla v^T \tag{3}$$

$$\sigma^* = \sigma + pI \tag{4}$$

Here σ^* refers to the deviatoric stress tensor, τ refers to the shear relaxation modulus which is a function of time, ε refers to the strain tensor, σ is the total stress, p is known as the hydrostatic pressure, and I refers to the unit tensor. The dimensionless relaxation modulus of a linear viscoelastic material, Prony series is developed as such:

$$R(t) = 1 - \sum_{i=1}^{N} \alpha_i \left(1 - e^{-\frac{t}{\beta_i}}\right) \tag{5}$$

Here, N, α_i, and β_i are material constants. Let's assume $c(t)$ is the creep function and $E(t)$ represents the relaxation function. In order to find the corresponding Prony series expression, $c(t)$ is to be transformed to $E(t)$. Following the theory of linear viscoelasticity, $c(t)$ and $E(t)$ are related as such:

$$1 = C(0)E(t) + \int_0^t E(t-s)\frac{dC(t)}{ds}\mathrm{ds} \tag{6}$$

$$\frac{1}{s^2} = \bar{C}(0)\bar{E}(t) \tag{7}$$

Inverse Laplace Transformation is applied to $E(t)$ from $C(t)$ in order to find $R(t)$, the dimensionless relaxation modulus.

Material Models

The challenge is to assign the right machanical properties to the major components of plaque such as necrtic core and fobrous cap.

(a) *Necrotic core* Necrotic core is conventionally considered to be isotropic and elastic. In the present study, it is assumed that necrotic core or lipid pool is incompressible with the Poisson's ratio of 0.49, and isotropic elastic, with a Young's modulus of 1 kPa.[15]

(b) *Fibrous cap* The fibrous cap tissue is assumed to be anisotropic and viscoelastic. Fibrous cap is a fiber-reinforced tissue due to the presence of collagen fibers which make the tissue stiffer and more resistant to fracture in the direction of fibers.[19] In this study, these fibers are

TABLE 1. Mechanical properties of fibrous cap,[17] θ represents the circumferential direction, r, the radial direction and z, the axial direction.

E_r (kPa) = E_z (kPa)	E_θ	$\nu_{r\theta}$	$\nu_{rz} = \nu_{\theta z}$	$G_{rz} = G_{r\theta} = G_{\theta z}$ (kPa)
100	1000	0.01	0.27	500

assumed to be aligned in the circumferential direction. In order to define mechanical properties to the fibrous cap tissue, a local cylindrical coordinate system is defined for the fibrous cap tissue and two principal directions of the radial and circumferential are defined. The assigned mechanical properties using this system are outlined in Table 1. To add viscoelastic behavior to fibrosis, two types of material behavior can be used; linear and nonlinear viscoelastic model. This study uses the linear model[19] in which creep and relaxation functions are only time dependent, i.e., stress is proportional to the strain at a given time

Using different arrangement of springs (elastic elements) and dashpots (viscous elements) linear viscoelastic behavior can be mathematically described which are known as the Maxwell Model, Kelvin–Voigt Model, Standard Linear Solid and Wiechert Model, as shown in Fig. 3.[19] This study employs the Wiechert Model to define viscoelastic behavior of fibrous cap, as it can more accurately match creep and relaxation behaviour of material in comparison with Standard Linear Solid. The Wiechert Model consists of a spring and a number (n) of Maxwell elements (i.e., series of spring and dashpot). (Table 2).

The constitutive equation of this model is developed as follows (σ, stress; ε, strain, E, elasticity modulus; η, viscosity or damping coefficient);

For a Wiechert model with one Maxwell arm:

$$\bar{\sigma}(s) = \left[E_e + E_m\left(\frac{s}{s+\frac{1}{\tau}}\right)\right]\frac{\varepsilon_0}{s} \tag{8}$$

By taking the inverse Laplace transform, the constitutive equation is developed as;

$$\sigma(t) = \left[E_e + E_m e^{-\frac{t}{\tau}}\right]\varepsilon_0 \tag{9}$$

And the relaxation modulus is defined as;

$$E(t) = \frac{\sigma(t)}{\varepsilon_0} = E_e + E_m e^{-\frac{t}{\tau}} \tag{10}$$

Using the Prony series, the relaxation modulus (Eq. 10) is modified for a Wiechert model with n Maxwell arms. Generally, the relaxation modulus is

TABLE 2. The constitutive equations developed for this model.

	Time domain	Laplace domain
Spring arm (elastic arm):	$\sigma_e = E_e\varepsilon$	$\bar{\sigma}_e(s) = E_e\bar{\varepsilon}(s)$
For each Maxwell arm:	$\dot{\varepsilon} = \frac{\dot{\sigma}_m}{E_m} + \frac{\sigma m}{\eta}$	$\bar{\sigma}_m(s) = E_m\left(\frac{s}{s+\frac{1}{\tau}}\right)\bar{\varepsilon}(s)$
	$\dot{\varepsilon} \doteq \frac{d\varepsilon}{dt}$, $\dot{\sigma} \doteq \frac{d\sigma}{dt}$	$\tau = \frac{\tau}{E_m}$
Total		$\sigma = \bar{\sigma}_e + \bar{\sigma}_m$

TABLE 3. Elements of time Prony series[19] as considered for the low viscoelastic model.

Index i	Relative module	Relaxation time
1	0.1595	0.001
2	0.1177	0.01
3	0.0623	0.1
4	0.1612	1
5	0.2101	10

obtained through shear relaxation data and the shear relaxation modulus are used in FE commercial codes. Thus, notation $E(t)$ is substituted with $G(t)$, where G_∞ is the fully relaxed shear modulus at time equal to infinity,

$$G(t) = G_\infty + \sum_{i=1}^{n} G_i e^{-\frac{t}{\tau}} \tag{11}$$

At t = 0;

$$G_0 = G_\infty + \sum_{i=1}^{n} G_i \tag{12}$$

Comparing Eqs. (11) with (12);

$$G(t) = G_0 - \sum_{i=1}^{n} G_i\left(1 - e^{-\frac{t}{\tau_i}}\right) \tag{13}$$

Dividing Eq. (13) by G_0 turns out (g(t), relative moduli at t; $\bar{g}_i^p$, relative relaxation moduli; τ_i relaxation time);

$$g_R(t) = 1 - \sum_{i=1}^{n} \bar{g}_i^p\left(1 - e^{-t/\tau_i}\right) \tag{14}$$

Elements of Eq. (14), also known as the Prony series model, are conventionally obtained by curve-fitting of stress-vs.-time data obtained in mechanical experiments on the material sample. Using stiffness matrix, D, the matrix form of Eq. (9) is defined as follows (D_0, instantaneous elasticity tensor or elasticity tensor at t = 0; ε, strain tensor;[19]

$$\begin{aligned}\sigma &= D(t)\varepsilon; D(t) = g_R(t)D_0 \\ &= \left(1 - \sum_{i=1}^{n} \bar{g}_i^p\left(1 - e^{-t/\tau_i}\right)\right)D_0\end{aligned} \tag{15}$$

Values of the Elements of matrix D_0 are outlined in Table 3. The material parameters used in the viscoelastic material model as applied to properties of plaque constituents are reported in Zareh *et al.*[19] In this study, an experimental–numerical technique to find parameters of a time Prony series with five spring-damper elements was performed. Table 3 outlines the values obtained in that study.

TABLE 4. Elements of time Prony series for plaque with high viscosity.

Index *i*	Relative module	Relaxation time
1	0.2233	0.001
2	0.1648	0.01
3	0.087	0.1
4	0.2257	1
5	0.2944	10

In this study, two viscoelastic models are considered; (1) a low viscoelastic model (Table 3), and (2) a high viscoelastic model (Table 4). The elements of Table 4 are modified so that the new model can represent the mechanical behavior of the fibrous cap tissue with high viscosity, which is caused by the high density of SMCs and monocytes inside the plaque. To reach this end, relative modules are increased by 40%.

It should be noted that the nature of lower viscoelastic behavior is closer to a pure elastic or hyperelastic material model.

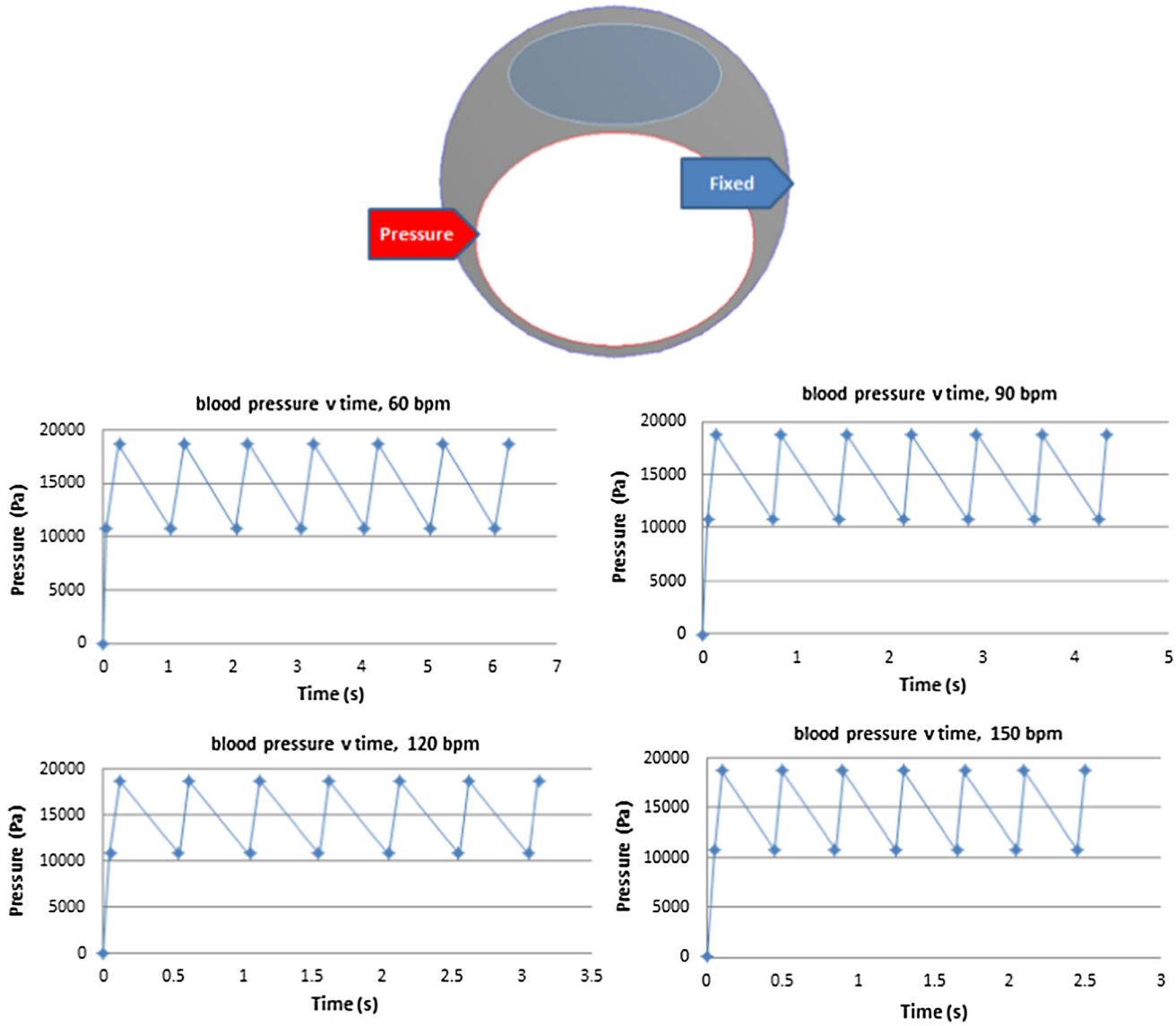

FIGURE 4. Illustration of the boundary conditions (top). Dynamic blood pressure in heart rates of 60, 90, 120, and 150 bpm. These graphs are used for the evaluation of HR effect on plaque vulnerability (bottom).

TABLE 5. Mesh independency study, the PCS for each model along with the number of elements used are shown in row A and B.

Models	1E	1F	1G
A			
PCS kPa	393	352	254
Elements	3411	4090	2949
B			
PCS kPa	391	348	250
Elements	6135	5216	6186
Comparison %	0.5	1.1	1.6

In row B, models were meshed with more elements in comparison with models in row A. Results show an acceptable range for discrepancy of PCS in each plaque model; thus, the mesh models employed in row A are sufficiently precise to be used for our computational approach. Also, results are time dependent due to time-dependency of the material properties and pressure. In this pre-study, results of PCS at $t = 0.2$ s have been considered for this comparison.

Boundary Conditions

Two types of boundary conditions (known variables) are used in this study: (1) Displacement, and (2) Load. Atherosclerotic plaque is circumscribed by the artery wall; thus, the outer wall of plaque is assumed to be fixed in all directions as the outer surface of plaque experiences negligible displacement in physiological condition.[19] Figure 5 illustrates this displacement boundary condition. Load in this study is referred to blood pressure. Given that the constitutive material models defined for the fibrous cap tissue is viscoelastic, the transmural pressure is considered the actual physiological blood pressure in the coronary arteries which is cyclic and time-dependent in nature. The numerical values related to the transmural pressure are outlined in Fig. 4.

Numerical Setup

FEM is employed in order to obtain the stress distribution and the PCS in the entire plaque section. The developed equation obtained for linear viscoelasticity of plaque properties were incorporated onto the commercially available FE code, ANSYS 2017. Geometrical models constructed in SolidWorks 2015 are carefully meshed by triangular elements so that a fine mesh was used in the critical area, i.e., the thin fibrous cap tissue between necrotic core and lumen. A mesh independent study is then performed in order to ensure of independency of results obtained from the modeling inputs.

After creating mesh *models*, ANSYS was used to discretize the governing equations. To find unknown nodal displacements and forces, these equations are solved under plane stress assumptions by Mechanical APDL 2018 running on an Intel® Core™ 2 Duo T6670 @ 2.2 GHz and 2.00 GB of RAM. It should be noted that the PCS values is considered the maximum value of von-Mises stresses calculated within the plaque for each condition.[19] Also, while common use in arterial wall mechanics for 2D modeling is plane-strain assumption as the artery's out-of-plane axial deformation is almost zero, this study utilizes plane-stress assumption. The plane-strain assumption is based on the fact that the vessel tissue is assumed to be incompressible and that the Poisson's ratio is nearly 0.5, i.e., the axial elongation due to the transmural pressure and the axial shrinkage due to radial expansion of the tissue are equal (hence, the plane-strain assumption) which is only applicable to conventional vessels with uniform cross sectional area. For the current study, it is safe to assume that the axial stress compared to the circumferential and radial stresses which are mainly responsible for plaque failure are trivial in a way stress in the axial direction is assumed to be zero, hence, the plane-stress assumption.

RESULTS AND DISCUSSION

Mesh Independency Study

Mesh independency of our results is of particular significance in this study which is done by performing further computation for each plaque model with higher mesh density. The mesh size is decreased until the point where by increasing the mesh density the results are not improved. The result of the mesh independency study is outlined in Table 5.

Figure 5 shows the values of PCS in three idealistic models with respect to HRs of 60, 90, 120, and 150 bpm. Two thicknesses (70 μm and 100 μm) and two viscoelastic models (low and high viscosities) are considered for the fibrous cap tissue. Results clearly indicate that HR noticeably affects the values of PCS. Moving from 60 bpm to 150 bpm when the cap thickness is set to 70 μm and a low viscosity is assigned to the fibrous cap tissue, the range of change in the PCS for the same model is 15–25 kPa. This range widens to 35–45 kPa when a high viscosity is assigned to the fibrous cap tissue (Fig. 4a). When the cap thickness is set to 100 μm, these ranges drop to 14–15 kPa for the low viscoelastic fibrous cap model and to 20–35 kPa for the high viscoelastic fibrous cap model (Fig. 4b). For the high viscoelastic fibrous cap model, the rate of change in the PCS values are higher to that of the low viscoelastic fibrous cap model as HR increases, assuming all other conditions, i.e., cap thickness, lumen maximum pressure, *etc.,* remain unchanged. Comparing the results outlined in Figs. 1a and 1b, there is evidence that if a higher viscosity is assigned to the fibrous cap tissue, lower values (15%) for PCS are obtained.

For the idealistic models of I1 and I3, the values of PCS drop as the cap thickness is set from 70 to 100 μm for both high and low viscoelastic fibrous cap models.

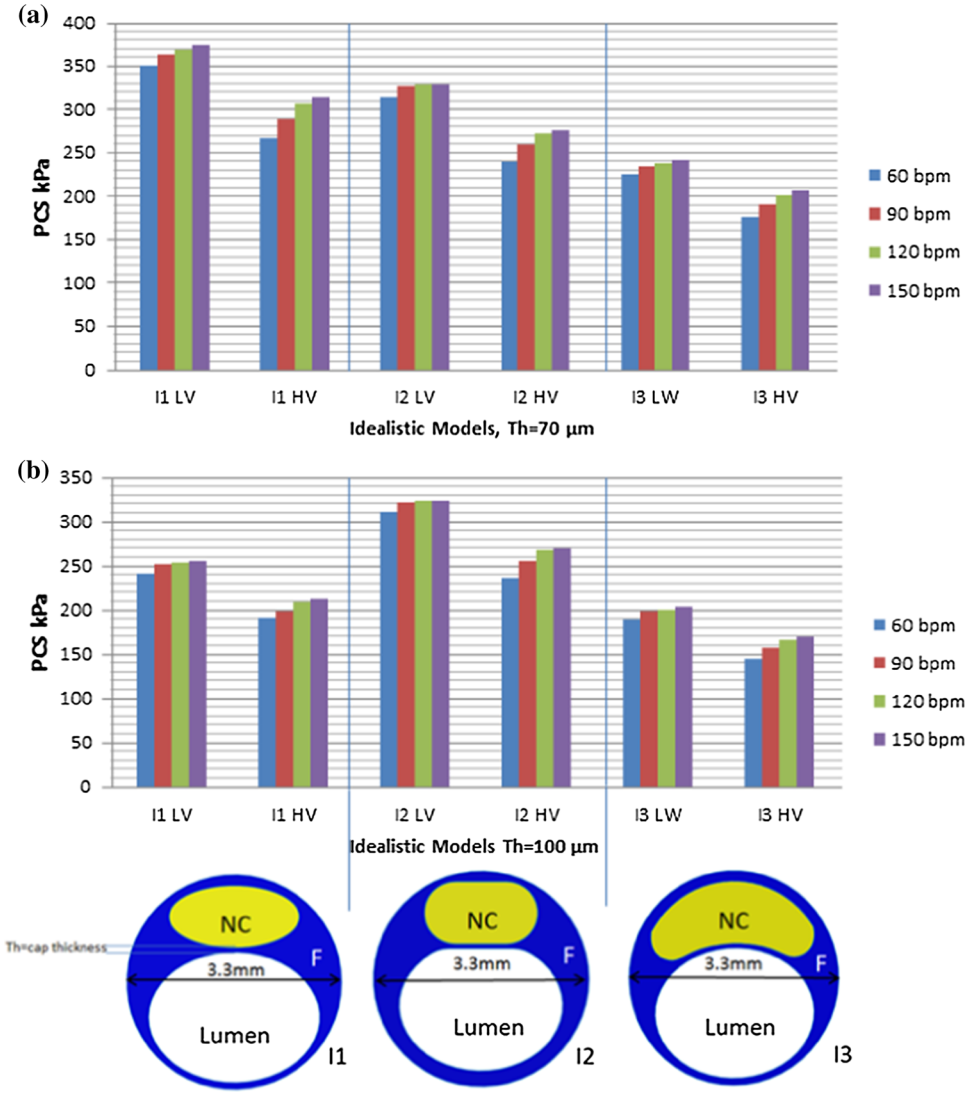

FIGURE 5. Illustration of idealistic geometrical models used and the values of PCS calculated in this study. I1, I2, and I3 are the 3 idealistic models, LV and HV refer to low and high viscous properties of the think fibrous cap tissue, respectively. (a) shows the values of PCS for the idealistic models when cap thickness is set to 70 μm, and (b) shows the values of PCS in the idealistic models when the cap thickness is set to 100 μm.

However, for the idealistic model of I2, regardless of the fibrous cap thickness (being 70 μm or 100 μm), the values of PCS remain in the same range with an error $< \sim 2\%$. Results obtained from I2 imply that the geometry of the plaque section and HR combined could be more influential on PCS than the thickness of the fibrous cap tissue alone.

The values of PCS under the same boundary conditions, i.e., dynamic lumen pressure and displacement boundary conditions, are shown in Fig. 6 for realistic models. Results further reinforce the hypothesis developed using the idealistic models that if a higher viscosity is assigned to the fibrous cap tissue, the values of PCS drops by ~ 15% and the effect of HR on PCS is higher.

Figure 7 demonstrates the increase in PCS with respect to that of when HR = 60 bpm discussed in Figs. 1 and 2 to better demonstrate the effect of viscoelasticity and HR on PCS. Results clearly show that jump in PCS from HR = 90 bpm to HR = 120 bpm is much higher than that of from 120 to 150 bpm in both low and high viscoelastic models. Depending on the severity of viscous models applied and HR, the values of PCS increase from 2% (in which HR = 90 bpm) to 18% (in which HR = 150 bpm).

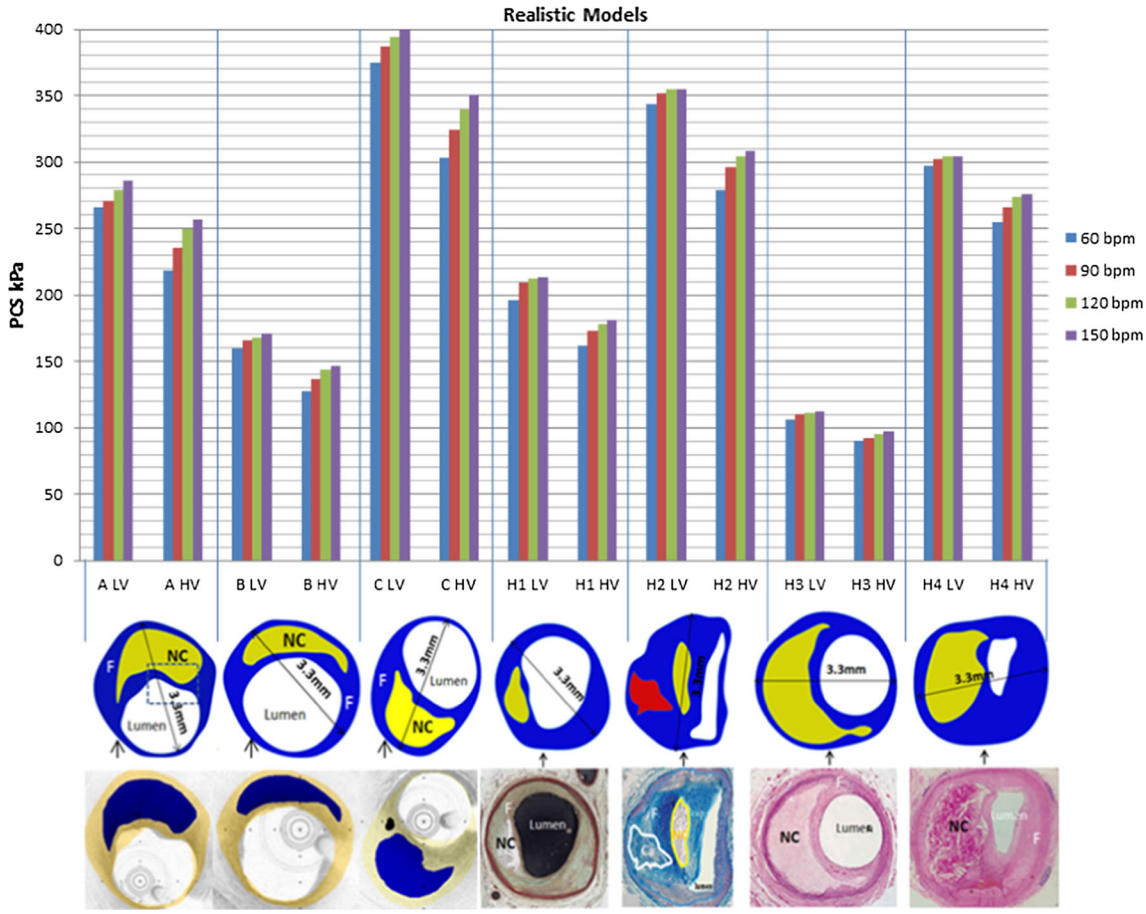

FIGURE 6. Illustration of patient-oriented geometrical models used in this study and their estimated PCS values through both HV and LV viscous materials; The imaging modalities used in this study are IVUS & OCT combined (models A, B, and C) and histology (models H1, H2, H3, and H4).[3,7,11] Blue, yellow and red in the digitized images refer to fibrous tissue, necrotic core and calcified regions, respectively.

CONCLUSION

Conditions of blood pressure in the majority of the hemodynamics computational and experimental studies are set according to a fixed HR of 72 bpm, which does not comprehensively represent the entire possible physiological hemodynamic conditions; such as, in resting status, sleeping status, *etc.,* where HR could be as low as 60 bpm. In contrast, jogging, running and emotional shocks could elevate HR to be as high as 150 bpm.

Besides, daily emotional conditions, such as stress and anxiety, may affect the HR. Therefore, a range of 60–150 bpm for HR seems to be reasonable normal HR conditions for cardiovascular related studies. In the current study, estimated PCS values within the plaque models with respect to HR variation and different viscoelastic models demonstrate the significance of HR and viscoelastic material model of the fibrous cap tissue for the assessment of atherosclerotic plaque vulnerability. As presence of smooth muscle cells (SMCs) and macrophages add viscoelastic behaviour to the fibrous cap tissue, the degree of viscoelasticity depends highly on plaque composition. The present results suggest that HR must be considered as a predictor for the mechanical instability of rupture-prone plaques, along with other factors such as cap thickness, necrotic core size and plaque morphology. Moreover, results evidently indicate impact of HR on vulnerability of plaque is strongly associated with the degree of tissue viscosity since higher viscosity in the fibrous cap tissue can intensify the effect of HR on PCS values (see Fig. 8). For example, in a standard Voigt Model, increased viscous properties of the plaque tissue lead to a longer lag between the transmural pressure and the corresponding tissue deformation (in this case plaque radial expansion). In contrast, lower viscosity causes the tissue to deform faster upon applying the trans-

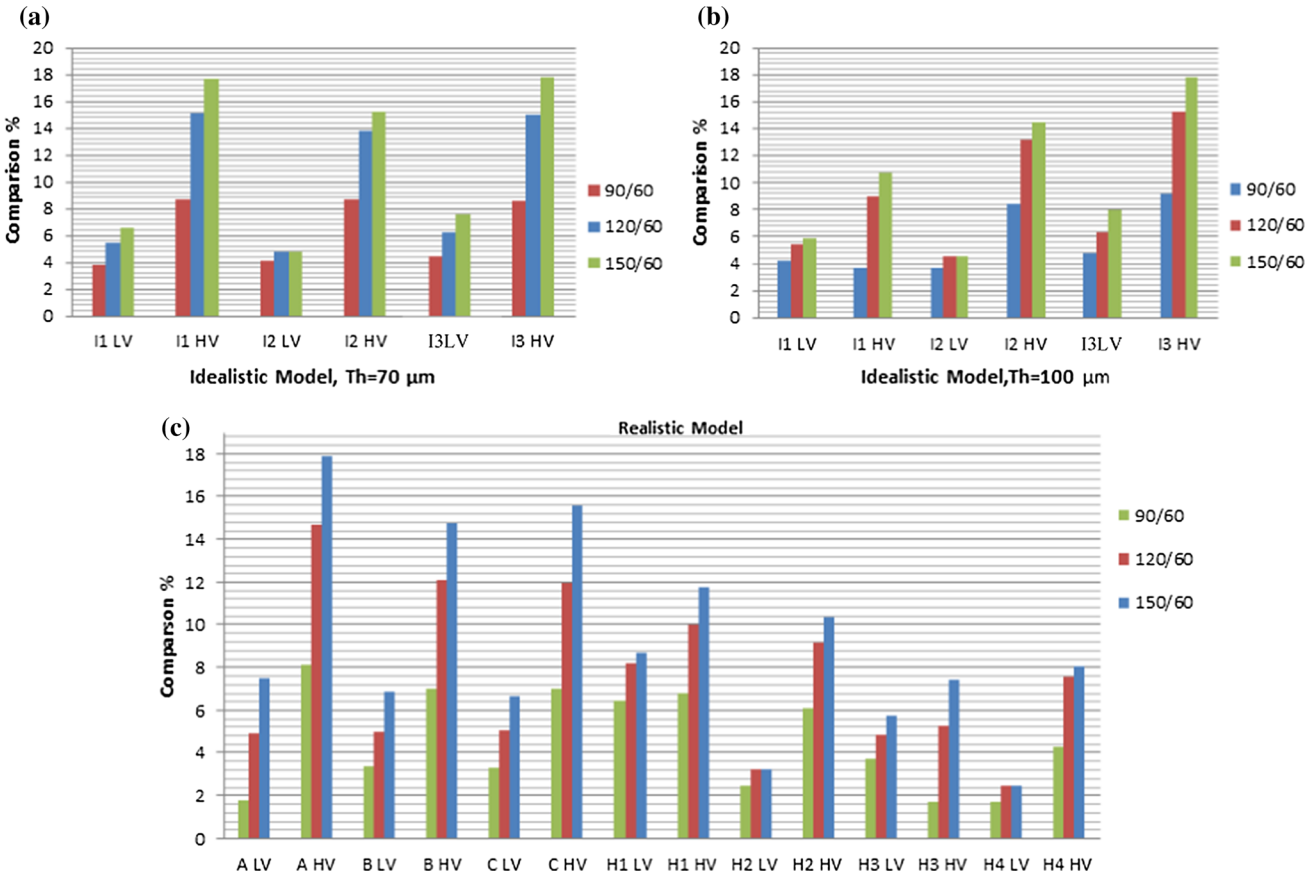

FIGURE 7. The comparison of values of PCS to that of obtained when HR = 60 bpm for idealistic and patient-oriented models. Two thicknesses and two viscoelastic models are considered for the idealistic models (Figs. 3a and 3b), and all patient-oriented models (Fig. 3c). LV and HV refer to low and high viscoelastic model for the fibrous cap tissue, respectively.

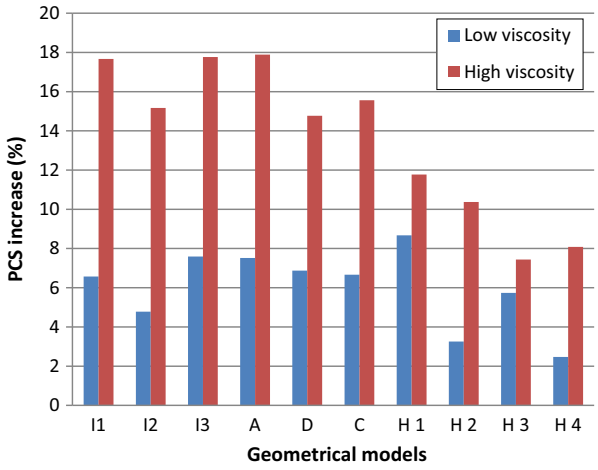

FIGURE 8. Increase in PCS values due to degree of viscoelasticity of the fibrous cap tissue and HR. Blue bar shows the increase in PCS moving from elastic model to low viscoelastic model for the fibrous cap tissue when HR = 60 bpm, red bar shows the increase in PCS moving from elastic model to high viscoelastic model for the fibrous cap tissue when HR = 150 bpm.

mural pressure. This lag can be translated to the increase of the apparent tissue elasticity in a way that PCS increases consequent to viscosity enlargement of the tissue based on the fact that the tissue deformation is considered the same. The apparent elasticity of the plaque tissue can be intensified by higher HR. As shown in Fig. 8, by keeping the elasticity of plaque unchanged, two cases were considered and PCS values were calculated for each case. In case 1, PCS values were compared in purely elastic and low viscoelastic models when HR was set to 60 Hz. In case 2, PCS values were compared in the pure elastic and high viscoelastic models when HR was set to 150 Hz. Case 1 study shows 9% increase in PCS, whereas in case two this increase reaches to 18%. Results strongly suggest that viscoelastic properties of the plaque tissue and HR together are important factors in the assessment of the detection of vulnerable plaques. Based on these results, any experimental methods assessing the viscoelasticity of plaque composition during progression are highly desirable.

ACKNOWLEDGMENTS

The authors acknowledge the University of British Columbia and NSERC (Discovery Grant) for financial support.

CONFLICT OF INTEREST

The authors declare that they have no conflict of interest.

REFERENCES

[1]Akyildiz, A., L. Speelman, H. Nieuwstadt, H. van Brummelen, R. Virmani, A. van der Lugt, *et al*. The effects of plaque morphology and material properties on peak cap stress in human coronary arteries. *Comput. Methods Biomech. Biomed. Eng*. 2015. https://doi.org/10.1080/10255842.2015.1062091.

[2]Akyildiz, A., L. Speelman, H. van Brummelen, M. Gutierrez, R. Virmani, A. van der Lugt, and F. Gijsen. Effects of intima stiffness and plaque morphology on peak cap stress. *Biomed. Eng. Online* 10(1):25, 2011. https://doi.org/10.1186/1475-925X-10-25.

[3]Bentzon, J. F., F. Otsuka, R. Virmani, and E. Falk. Mechanisms of plaque formation and rupture. *Circ. Res.* 114(12):1852–1866, 2014.

[4]Cardoso, L., A. Kelly-Arnold, N. Maldonado, D. Laudier, and S. Weinbaum. Effect of tissue properties, shape and orientation of microcalcifications on vulnerable cap stability using different hyperelastic constitutive models. *J. Biomech*. 47(4):870–877, 2014. https://doi.org/10.1016/j.jbiomech.2014.01.010.

[5]Casscells, W., M. Naghavi, and J. Willerson. Vulnerable atherosclerotic plaque—a multifocal disease. *Circulation* 107(16):2072–2075, 2003. https://doi.org/10.1161/01.cir.0000069329.70061.68.

[6]Cilla, M., E. Peña, and M. A. Martínez. 3D computational parametric analysis of eccentric atheroma plaque: Influence of axial and circumferential residual stresses. *Biomech. Model. Mechanobiol*. 11(7):1001–1013, 2012. https://doi.org/10.1007/s10237-011-0369-0.

[7]Farb, A., A. Burke, A. Tang, Y. Liang, P. Mannan, J. Smialek, *et al*. Coronary plaque erosion without rupture into a lipid core—A frequent cause of coronary thrombosis in sudden coronary death. *Circulation* 93(7):1354–1363, 1996.

[8]Fayad, Z. Computed tomography and magnetic resonance imaging for noninvasive coronary angiography and plaque imaging: current and potential future concepts. *Circulation* 106(15):2026–2034, 2002. https://doi.org/10.1161/01.cir.0000034392.34211.fc.

[9]Fuster, V., P. Moreno, Z. Fayad, R. Corti, and J. Badimon. Atherothrombosis and high-risk plaque part I: Evolving concepts. *J. Am. Coll. Cardiol*. 46(6):937–954, 2005. https://doi.org/10.1016/j.jacc.2005.03.074.

[10]Heiland, V. M., C. Forsell, J. Roy, U. Hedin, and T. C. Gasser. Identification of carotid plaque tissue properties using an experimental-numerical approach. *J. Mech. Behav. Biomed. Mater*. 27:226–238, 2013.

[11]Huang, X., C. Yang, J. Zheng, R. Bach, D. Muccigrosso, P. Woodard, and D. Tang. Higher critical plaque wall stress in patients who died of coronary artery disease compared with those who died of other causes: A 3D FSI study based on ex vivo MRI of coronary plaques. *J. Biomech*. 47(2):432–437, 2014. https://doi.org/10.1016/j.jbiomech.2013.11.007.

[12]Hurst, J. In Hurst's the heart (13th ed.). New York: McGraw-Hill Medical, 2011.

[13]Kiousis, D., S. Rubinigg, M. Auer, G. Holzapfel, and Hållfasthetslära (Inst.), Skolan för teknikvetenskap (SCI). Biomekanik. A methodology to analyze changes in lipid core and calcification onto fibrous cap vulnerability: the human atherosclerotic carotid bifurcation as an illustratory example. *J. Biomech. Eng.-Trans. ASME* 131(12):121002, 2009. https://doi.org/10.1115/1.4000078.

[14]Mohammadi, H., and K. Mequanint. An inverse numerical approach for modeling aortic heart valve leaflet tissue oxygenation. *J. Cardiovasc. Eng. Technol*. 3(1):73–79, 2012.

[15]Mohammadi, H., and K. Mequanint. Effect of stress intensity factor in evaluation of instability of atherosclerotic plaque. *J. Mech. Med. Biol*. 2014. https://doi.org/10.1142/s0219519414500729.

[16]Ohayon, J., G. Finet, A. M. Gharib, D. A. Herzka, P. Tracqui, J. Heroux, and R. I. Pettigrew. Necrotic core thickness and positive arterial remodeling index: Emergent biomechanical factors for evaluating the risk of plaque rupture. *Am. J. Physiol. Heart Circ. Physiol*. 295(2):717–727, 2008. https://doi.org/10.1152/ajpheart.00005.2008.

[17]Ohayon, I., G. Finet, F. Treyve, G. Rioufol, and O. Dubreuil. A three-dimensional finite element analysis of stress distribution in a coronary atherosclerotic plaque: in vivo prediction of plaque rupture location. In: Biomechanics applied to computer assisted surgery, edited by Y. Payan. Trivandrum: Research Signpost, 2005, pp. 225–241.

[18]Veress, A. I., J. F. Cornhill, K. A. Powell, E. E. Herderick, and J. D. Thomas. Finite element modeling of atherosclerotic plaque. In Paper presented at the Proceedings of computers in cardiology conference, pp. 791–794. 1993. https://doi.org/10.1109/cic.1993.378366.

[19]Zareh, M., G. Fradet, G. Naser, and H. Mohammadi. Are two-dimensional images sufficient to assess the atherosclerotic plaque vulnerability: a viscoelastic and anisotropic finite element model. *Cardio. Vasc. Syst*. 3(1):3, 2015. https://doi.org/10.7243/2052-4358-3-3.